Regulate Upconversion Effect to Promote Removal of Biofilms on Titanium Surface via Photoelectrons

Kai Wang,[a] Yufei Tang,[b] Keyi Yao,[a] Shuqi Feng,[b] Bingfeng Wu,[b] Lin Xiang,*[b] Xuemei Zhou*[a]

[a] School of Chemical Engineering, Sichuan University, Chengdu 610065, China. Email: xuemeizhou@scu.edu.cn.

[b] State Key Laboratory of Oral Diseases & National Center for Stomatology & National Clinical Research Center for Oral Diseases, West China Hospital of Stomatology, Sichuan University, Chengdu 610041, Sichuan, China. E-mail: dentistxiang@126.com.

Contents

Table S1. Experimental conditions to prepare different samples.

Samples	Au sputtering time (min)	RE deposition time (h)	Concentration of Yb^{3+} (%)	Concentration of Er^{3+} (%)
TiO_2	0	0	0	0
Au_{α}-$RE_1(Yb_{20}$-$Er_2)/TiO_2$	α=0, 1, 3	1	20	2
Au_1-$RE_{\beta}(Yb_{20}$-$Er_2)/TiO_2$	1	β=0, 1, 3	20	2
Au_1-$RE_1(Yb_{\gamma}$-$Er_2)/TiO_2$	1	1	γ=0, 20, 40	2
Au_1-$RE_1(Yb_{20}$-$Er_{\delta})/TiO_2$	1	1	20	δ=0, 2, 4

Table S2. Atomic percentage (at. %) of different samples according to high-resolution XPS spectra of different elements.

Samples/Elements	C	O	F	Na	Ti	Au	Y
Au_1-$RE_1(Yb_{20}$-$Er_2)/TiO_2$	31.4	21.4	**28.5**	**4.1**	4.3	**6.3**	**4.1**
Au_3-$RE_1(Yb_{20}$-$Er_2)/TiO_2$	28.4	20.5	21.9	3.6	6.3	**12.4**	6.9
$RE_1(Yb_{20}$-$Er_2)/TiO_2$	25.5	40.8	**12.1**	**3.3**	16.4	0	**1.9**
Au_1-$RE_3(Yb_{20}$-$Er_2)/TiO_2$	27.6	14.3	**33.7**	**5.5**	4.0	9.0	**7.4**
Au_1/TiO_2	29.5	33.5	0	0	16.6	20.4	0

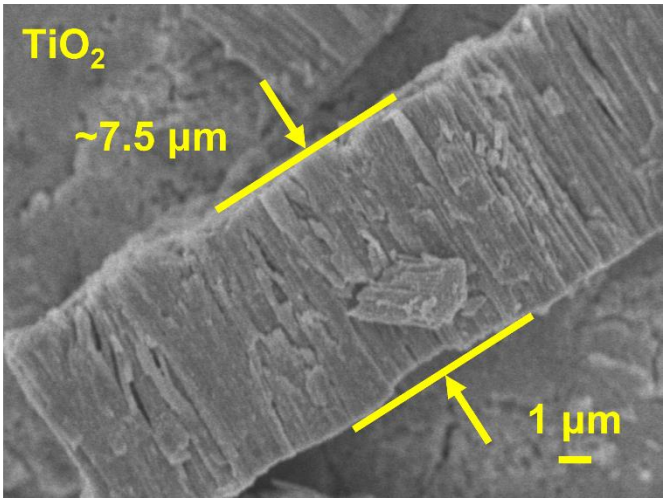

Fig. S1. SEM image of side view of TiO_2.

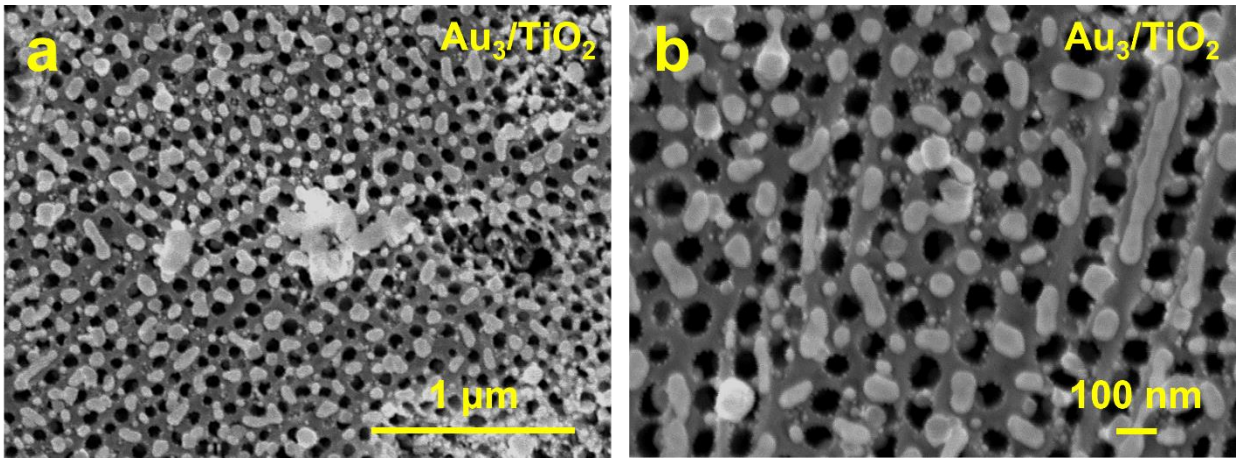

Fig. S2. SEM images of Au_3/TiO_2 in (a) overview and (b) close observation.

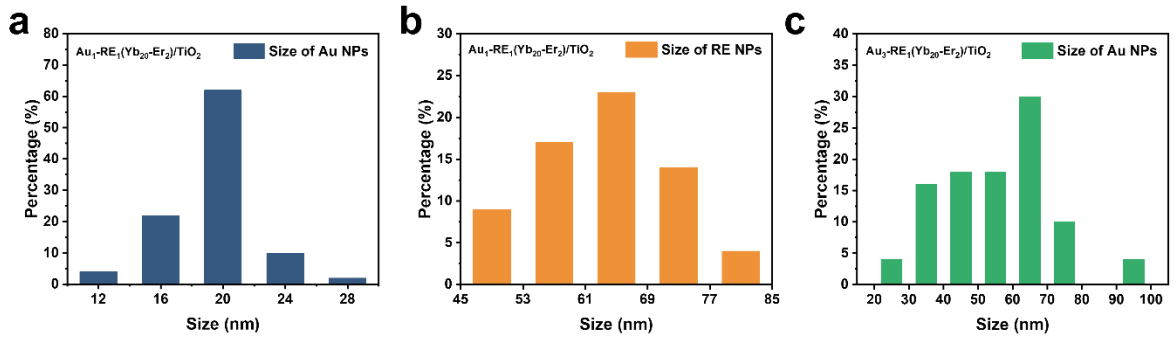

Fig. S3. Analysis on the size distribution of (a) Au NPs (20±3 nm) and (b) RE NPs (64±9 nm) for Au_1-$RE_1(Yb_{20}$-$Er_2)/TiO_2$. (c) Analysis on the size distribution of Au NPs for Au_3-$RE_1(Yb_{20}$-$Er_2)/TiO_2$ (55±16 nm).

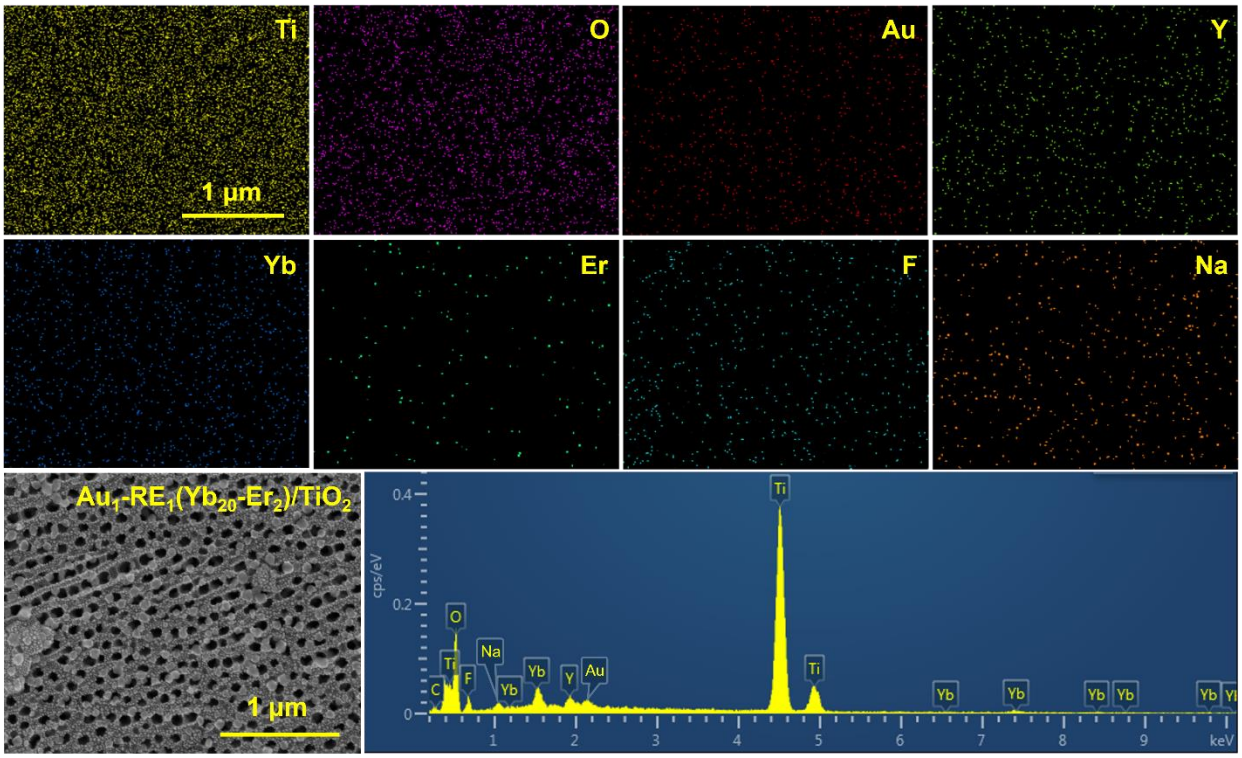

Fig. S4. EDS mapping of Au_1-$RE_1(Yb_{20}$-$Er_2)/TiO_2$.

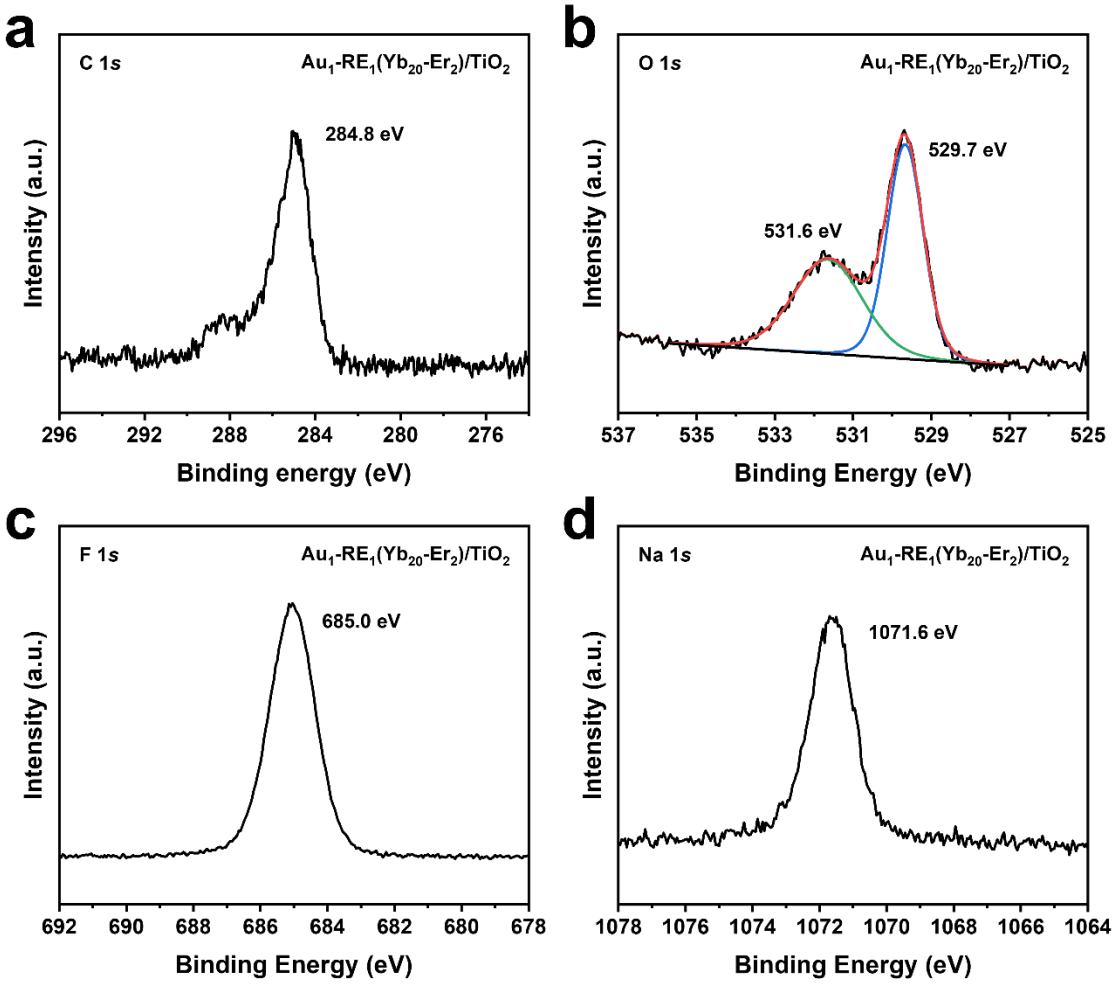

Fig. S5. XPS spectra of (a) C 1*s*, (b) O 1*s*, (c) F 1*s*, and (d) Na1*s*. Au_1-$RE_1(Yb_{20}$-$Er_2)/TiO_2$.

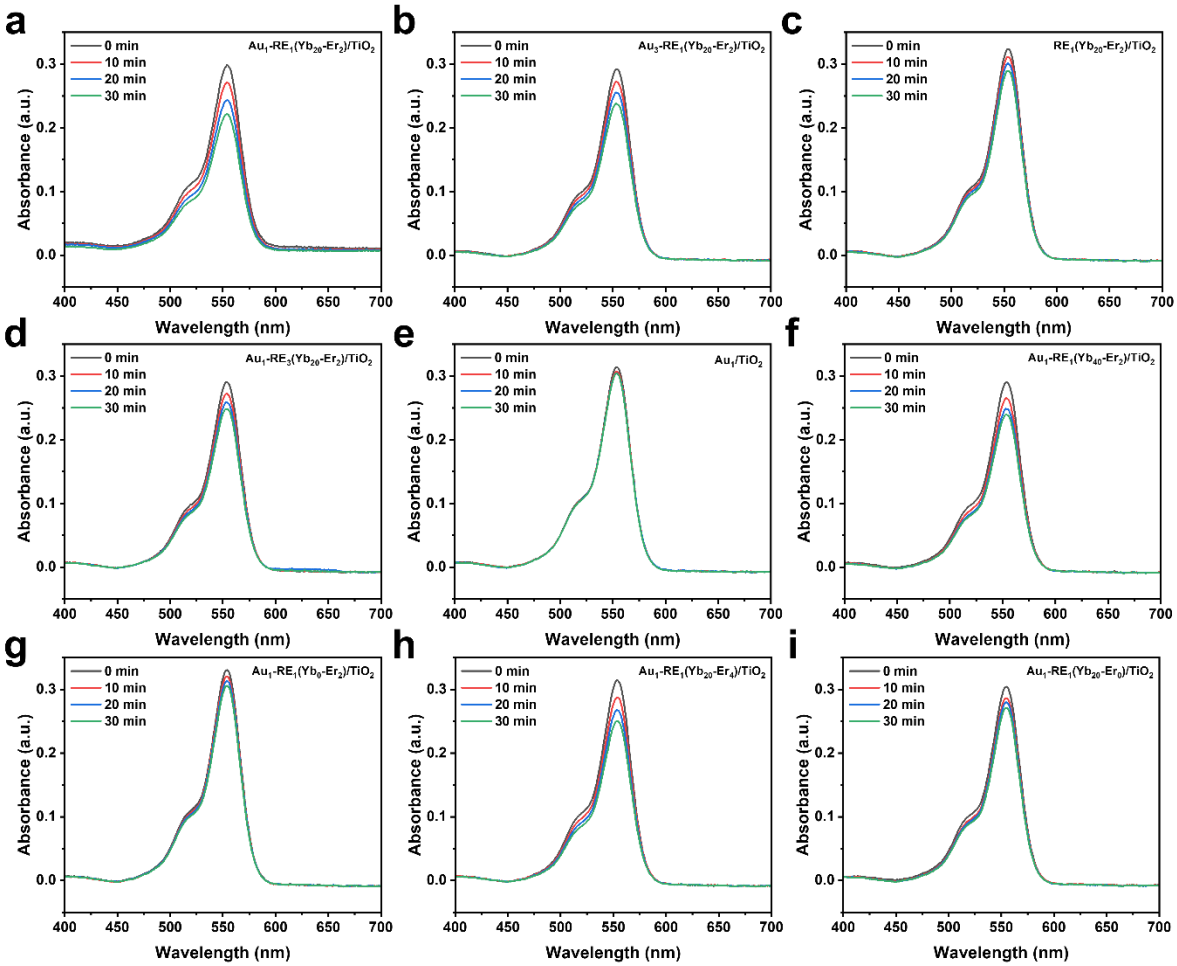

Fig. S6. The degradation curve of RhB for different samples under NIR irradiation: (a) Au_1-$RE_1(Yb_{20}$-$Er_2)/TiO_2$ (b-c) different Au loading, (d-e) different RE deposition amount, (f-g) different concentration of Yb^{3+}, (h-i) different concentration of Er^{3+}.

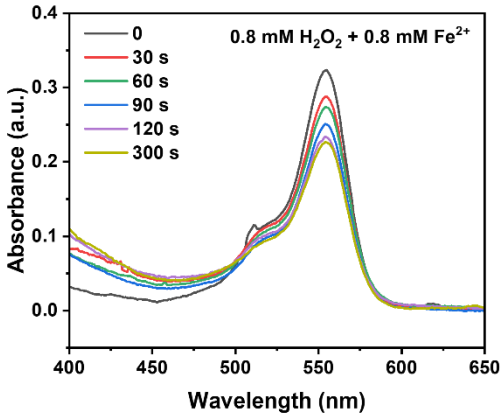

Fig. S7. Absorbance of RhB aqueous solution measured over time, catalyzed by Fe^{2+} (0.8 mM) and H_2O_2 (0.8 mM).

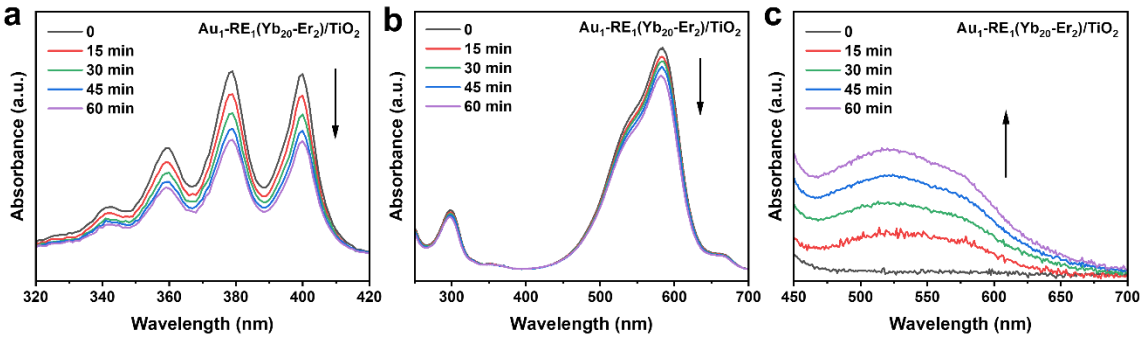

Fig. S8. UV-vis absorbance spectra of (a) ADBA and (b) MV for Au_1-$RE_1(Yb_{20}$-$Er_2)/TiO_2$ under NIR irradiation. (c) Absorbance of NBT solution with Au_1-$RE_1(Yb_{20}$-$Er_2)/TiO_2$ under NIR irradiation.

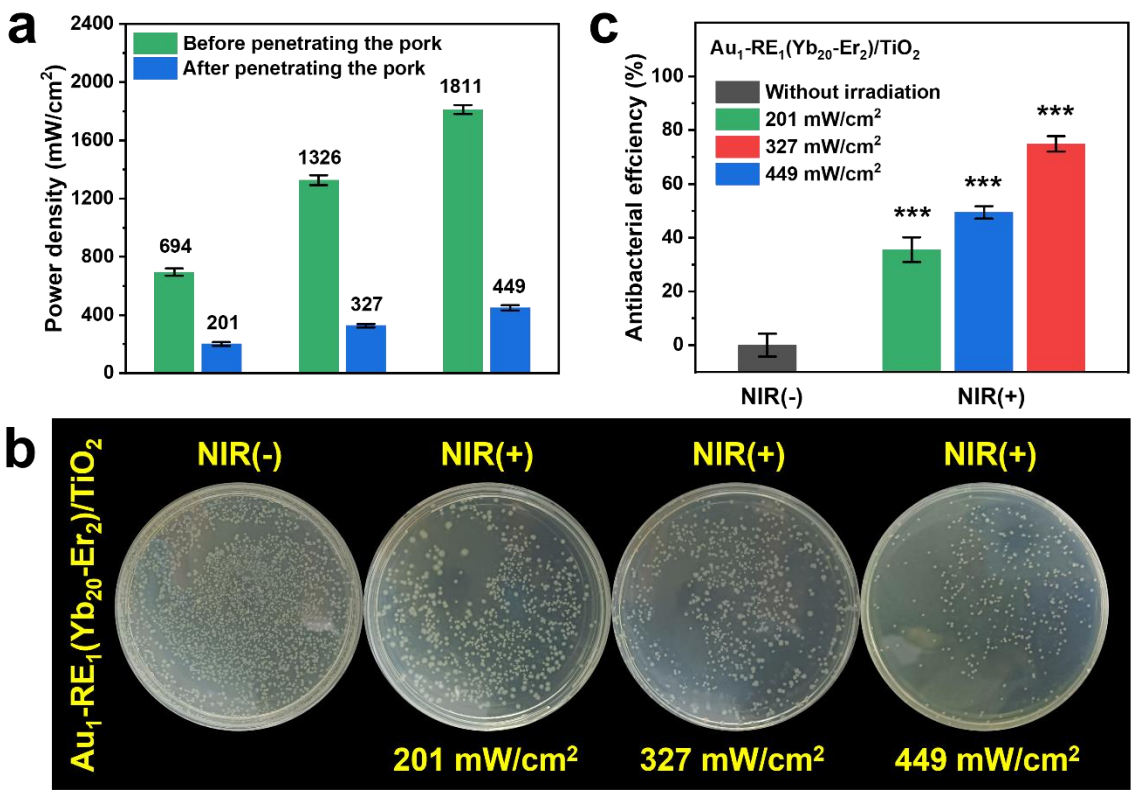

Fig. S9. (a) Penetration ability of the 980 nm laser in 3 mm thick pork. (b) and (c) Antibacterial effect of NIR with different power density after penetrating 3 mm thick pork. The statistics were presented as means ± S. D., n=3, * $p<0.05$, ** $p<0.01$, *** $p<0.001$, and ns (not significant).

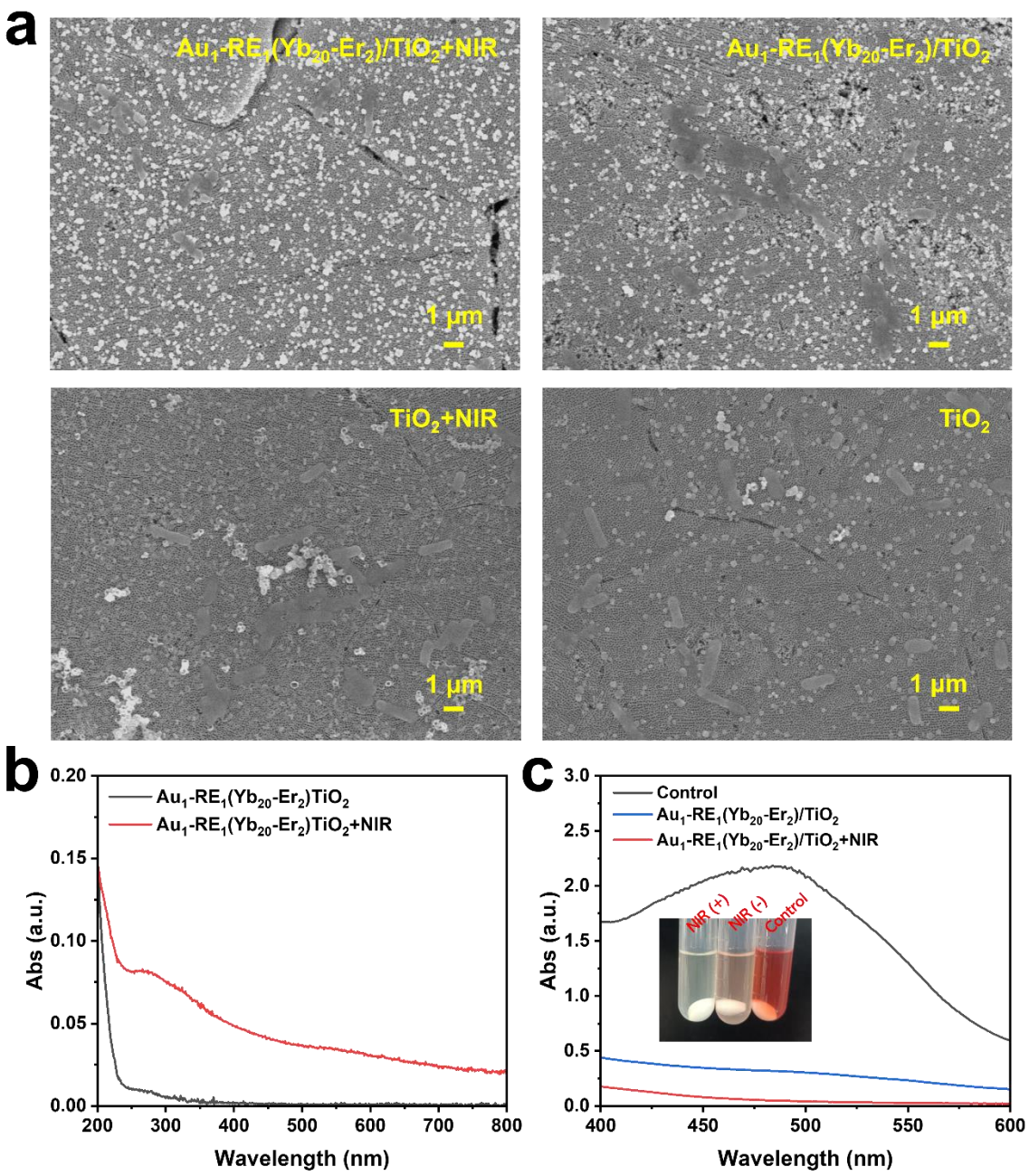

Fig. S10. (a) SEM images of *E. coli* of Au_1-$RE_1(Yb_{20}$-$Er_2)/TiO_2$ and TiO_2 under NIR irradiation or dark. (b) The release of nucleic acid and protein from *E. coli* of Au_1-$RE_1(Yb_{20}$-$Er_2)/TiO_2$ group under NIR irradiation or dark. (c) The absorption curves of *E. coli* of control and Au_1-$RE_1(Yb_{20}$-$Er_2)/TiO_2$ mixed with INT solution under NIR irradiation or dark.

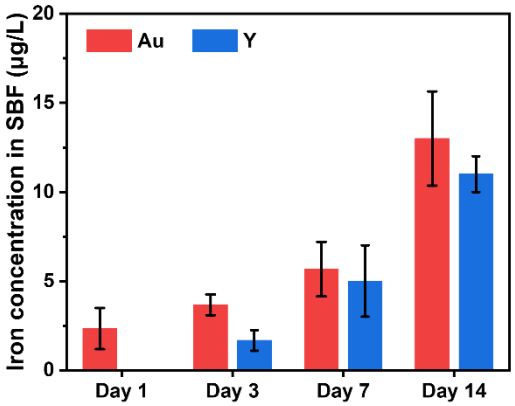

Fig. S11. Release of Au and Y ions from Au_1-$RE_1(Yb_{20}$-$Er_2)/TiO_2$ in SBF solution, detected on day 1, 3, 7, and 14.